

Liquid–Liquid Equilibrium for Ionic Liquid Systems Using COSMO-RS: Effect of Cation and Anion Dissociation

Tamal Banerjee

Dept. of Chemical Engineering, Indian Institute of Technology, Guwahati, India

Kaushal Kishore Verma and Ashok Khanna

Dept. of Chemical Engineering, Indian Institute of Technology, Kanpur, India

DOI 10.1002/aic.11495

Published online April 22, 2008 in Wiley InterScience (www.interscience.wiley.com).

Ionic liquids with their limitless combination of cations and anions can offer an optimal solvent for a specific purpose. But not all corresponding experimental studies are possible as they will be time consuming and expensive. A judicious screening of the various possible solvents is required to select the proper ionic liquid. Conductor-like screening model (COSMO) along with its extension to real solvents can be used for these predictions. In this work, modified version COSMO_LL has been used to predict the liquid–liquid equilibria (LLE) for 32 ternary systems, available in literature, each having an ionic liquid. A complete dissociation of cations and anions of the ionic liquid has been assumed. The root mean square deviation for all these systems is ~9% which is excellent when compared with ~50% obtained for predictions using the nondissociated composite molecule. Additionally, experimental LLE data has been collected for four ternary systems, namely: (a) 1-ethyl-3-methylimidazolium ethylsulphate [Emim] [EtSO₄] – Ethanol-Hexene, (b) 1-ethyl-3-methylimidazolium ethylsulphate [Emim] [EtSO₄] – Ethanol-Heptene, (c) 1,2-dimethyl-3-ethylimidazolium ethylsulphate [E-2,3-dmim] [EtSO₄] – Ethanol-Hexene, and (d) 1,2-dimethyl-3-ethylimidazolium ethylsulphate [E-2,3-dmim] [EtSO₄] – Ethanol-Heptene. The tie lines have been estimated using NMR and these have been compared with COSMO_LL predictions giving an average rmsd of ~6%.

© 2008 American Institute of Chemical Engineers AIChE J, 54: 1874–1885, 2008

Keywords: COSMO-RS, ionic liquids, liquid–liquid equilibria, activity coefficients

Introduction

Ionic liquids are attractive solvents as they are nonvolatile, inflammable, and have a high thermal stability. They provide a highly solvating and noncoordinating medium in which a variety of organic and inorganic solutes are able to dissolve. Recently much work has been carried out to predict the phase equilibrium of ionic liquids. These liquids, owing to

their negligible vapor pressure and a limitless possible combinations of cations and anions, have been used as a replacement^{1,2} for volatile organic solvents. Earle et al.³ recently distilled ionic liquid without decomposition at very low pressures. In their pioneering work they were successful in distilling the trifluoromethanesulphonylimide [(CF₃SO₂)₂N] based ionic liquids at 100 Pa and 573 K without decomposition. An excellent review of the phase equilibria properties of ionic liquids is given by Heintz.⁴ Some recent data exist for the ternary liquid–liquid equilibria (LLE) systems involving ionic liquids: for the separation of aromatic-aliphatic,^{5–11} alcohol-ether,^{12–14} and alcohol-aliphatic^{15,16} mixtures using ionic liquids as solvents. Recently, extraction of citrus essen-

This article contains supplementary material available via the Internet at <http://www.interscience.wiley.com/jpages/0001-1541/suppmat>.

Correspondence concerning this article should be addressed to A. Khanna at akhanna@iitk.ac.in.

tial oil terpenless was studied using the ionic liquid 1-ethyl-3-methylimidazolium ethylsulphate.^{17,18} The same ionic liquid was also used to purify gasoline octane boosters.¹⁹

The reported tie line data have been correlated using the excess Gibb's free energy models such as NRTL²⁰ and UNIQUAC.²¹ These models use the activity coefficients, which require proper binary interaction parameters that can represent LLE for highly nonideal liquid mixtures. The obtained parameters are not unique, thereby having limited global applicability. In case no experimental LLE data for the systems of interest are available, the infinite dilution activity coefficients can be used for parameter estimation but at the cost of accuracy. Thus a need was felt to directly predict the tie-line data, which can have global applicability. Continuum Solvation Model such as CONductor-like Screening Model (COSMO) along with its extension to real solvents (RS) is one model used for such predictions. This model, in principle, can be used to determine the chemical potential of any species in a mixture from quantum mechanical calculations.

The COSMO has been described in the work of Klamt and Schüürmann.²² In COSMO-RS, molecules are treated as a collection of surface segments and an expression for the chemical potential of segments in the condensed phase is derived in which interaction energies between segments are calculated. The chemical potential of each molecule is then obtained by summing the contributions of the segments. The extension to RS is given in excellent papers by Klamt.^{23–26} Variants of COSMO-RS have also evolved thereon, which include the COSMO-SAC²⁷ and COSMO-RS (OI)²⁸ models.

The expressions and methodology are given in detail in our previously published work on COSMO-RS.^{29–31} Modified versions of this model, COSMO_VL and COSMO_LL, have been used to predict the vapor–liquid equilibria (VLE),²⁹ LLE,³⁰ and infinite dilution activity coefficients (γ_i^∞).³¹ We will be using the COSMO_LL model for the prediction of LLE of ionic liquid based ternary systems. Recently, LLE has been predicted using COSMO-RS for binary systems of 1,3-dialkylimidazolium-based ionic liquid + hydrocarbon.³²

In this work, LLE has been predicted for ternary systems based on 12 ionic liquids. These ionic liquids are based on one of the seven cations: 1-methyl-3-methylimidazolium [Mmim], 1-ethyl-3-methylimidazolium [Emim], 1-butyl-3-methylimidazolium [Bmim], 1-hexyl-3-methylimidazolium [Hmim], 1-octyl-3-methylimidazolium [Omim], 1,2-dimethyl-3-ethylimidazolium [E-2,3-Mim], 1-butyl-3-methylpyridinium [Bmpy] and one of the eight anions namely: chloride[Cl], tetrafluoroborate [BF₄], hexafluorophosphate [PF₆], methylsulphate [CH₃SO₄], ethylsulphate [EtSO₄], octylsulphate [C₈H₁₇SO₄], diethyleneglycolmonomethylethersulphate [MDEG], and trifluoromethane sulphonate [CF₃SO₃].

Computational Details

The Quantum Chemistry Package of Gaussian 03³³ has been used to compute the COSMO files. The first step for COSMO-RS calculation is to estimate the sigma profile of each species. The equilibrium geometry of the cations and anions in the ideal gas phase are first obtained separately using the density functional theory PBV86.³⁴ The Triple Zeta Valence Potential³⁵ basis set has been used in combination with the density fitting basis set DGA1.³⁶ The ideal screening

Table 1. Cavity Radii Values Considered for Our Work

Element	Radius (Å)
H	1.30
C	2.00
N	1.83
O	1.72
F	1.72
S	2.16
Cl	2.05
Br	1.85
I	1.98
P	2.10

charges on the molecular surface are then computed using the same level of theory [PBV86]. The radii of the elements are used to define the cavity for the molecule. The radii of the nine components are reported in Table 1. For phosphorous a default value of $1.17 R_{\text{Bondii}}$ ^{37,38} has been used.

For the isolated cation and anion, initial geometry optimization was done using Hartree-Fock³⁹ level of theory. For the cation, a stepping stone approach was used, starting with the imidazolium ring and adding successive carbons until the desired cation was constructed. It was found from previous studies by Turner et al.⁴⁰ that the imidazolium ring has a planar structure. Frequency optimization was done at the same level on the optimal cation geometry in order to detect the presence of any imaginary or negative frequencies. The absence of negative vibrational frequencies verified the existence of a true minimum. A similar approach for anion has been taken with the exception of stepping stone approach. In the case of [Bmim] cation and [PF₆] anion, we have compared the final optimized energy with the values reported by Meng et al.⁴¹ The values obtained using the HF/6-31G* level of theory: -420.382300 and -937.602709 Hartrees compare very well with our values of -420.382305 and -937.602689 Hartrees, respectively. The values for other ions were not available for comparison. Thereafter, the final optimized structure was taken for the generation of COSMO file using GAUSSIAN03 by PBV86 density functional theory.

For the generation of composite molecule, the geometry optimization has been done on GAUSSIAN03 via the visualization software MOLDEN.⁴² In this visualization software, the optimized isolated cation and anion structures obtained, as discussed earlier, have been initially connected using a dummy atom. The dummy atom has nothing to do with the final optimized structure. Once the optimization loop starts, the dummy atom drops off and the cation and anion adjust within the optimized structure. Initially, the anion is placed randomly on top of the cation in all possible orientations. The structure having the least total energy is then used for COSMO file generation. Similar approach has also been adopted by Meng et al.⁴¹ The final optimized energy for [Bmim] [PF₆] is -1358.115640 Hartrees, which compares well with the reported value of -1358.115644 Hartrees.

The selection of the optimized structure is the most important part in generating the COSMO file/sigma profile. A key assumption for the generation of COSMO file is that each molecule is at a global energy minimum after the geometry optimization. To ensure that the molecule is at global minimum, we have

(a) performed a frequency analysis on the optimized structure and ensured that all the frequencies are positive, and

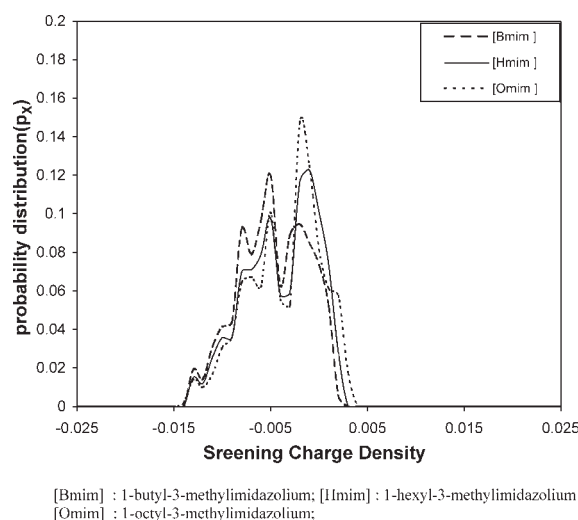


Figure 1. Sigma profiles for cations.

(b) compared the final optimized energy for the composite molecule as well as for cation and anion with the reported values.

In our work, we have adopted both approaches: composite molecule as well as dissociated cation/anion. However, for dissociated cation/anion, we could match the values for [Bmim] and PF_6 only as the values for other cations/anions were not available. We have adopted this process and assumed the structure is at global minimum when the above two conditions (a) and (b) are satisfied.

Sigma Profiles and Sigma Potentials of Cations and Anions

The sigma profiles and potentials for cations are shown in Figures 1 and 2, respectively. A small part of the normalized sigma profiles lie to the left of the hydrogen bonding cutoff radius (i.e., $\sigma < -0.0082 \text{ e}/\text{\AA}^2$), indicating hydrogen bonding donor capacity. The sigma profiles for [Bmim], [Hmim], and [Omim] are of the same nature. Most of the prominent peaks lie on the negative side of the sigma profile: e.g., $-0.001 \text{ e}/\text{\AA}^2$

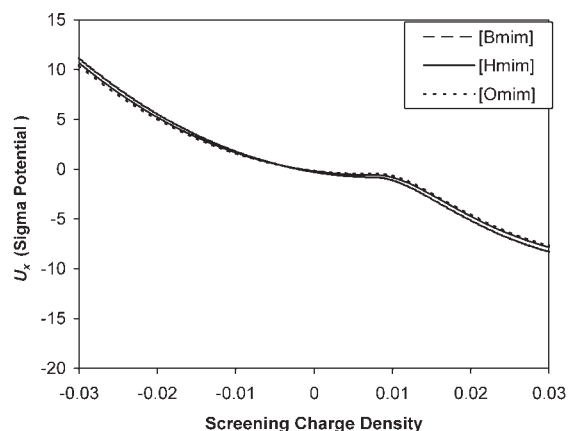


Figure 2. Sigma potentials for cations.

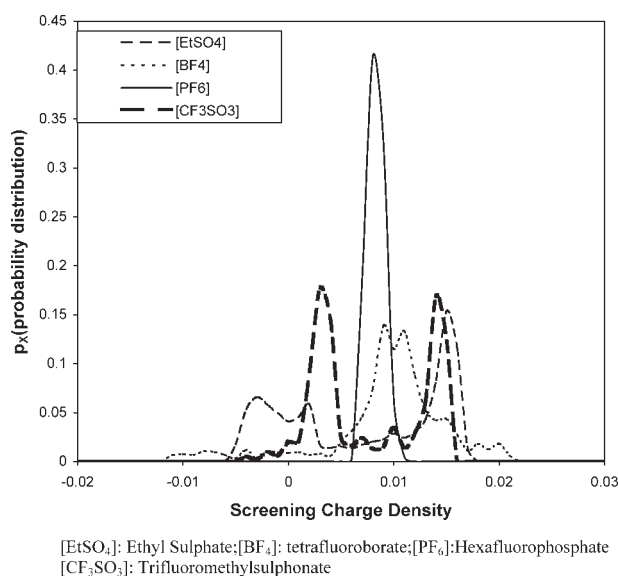


Figure 3. Sigma profiles for anions.

for [Hmim] and [Omim], $-0.0018 \text{ e}/\text{\AA}^2$ for [Bmim]. These negative screening charges are due to the positive charge residing inside the imidazolium ring. All the three cations [Bmim], [Hmim], [Omim] also show peaks at the outmost position in the negative direction. This effect also shows up in the sigma potential (Figure 2), i.e., negative values of chemical potentials are encountered on the positive side of the screening charge densities (SCDs). The negative values are encountered since extra free energy is gained by forming hydrogen bonds. It should be noted that extra energy is gained with the formation of hydrogen bonds, which is negative in value when compared with the free energy required (which is positive in nature) for removing the SCDs.

The sigma profiles and potentials for anions are shown in Figures 3 and 4, respectively. For all the anions, peaks lie on the right of the cutoff zone for hydrogen bonding, i.e.,

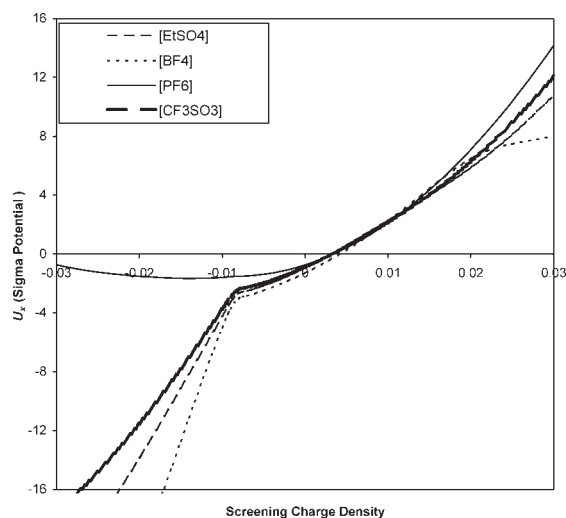


Figure 4. Sigma potentials for anions.

Table 2. Comparison of COSMO-XX Parameters

Parameter	COSMO-RS ²⁵	COSMO_VL ²⁹	COSMO_LL ³⁰
A_{eff}	6.25 Å ²	7.55 Å ²	6.32 Å ²
α'	8896 (kcal Å ⁴)/(mol e ²)	5950 (kcal Å ⁴)/(mol e ²)	8419 (kcal Å ⁴)/(mol e ²)
c_{hb}	54,874 (kcal Å ⁴)/(mol e ²)	83,690 (kcal Å ⁴)/(mol e ²)	75,006 (kcal Å ⁴)/(mol e ²)
σ_{hb}	0.0085 e/Å ²	0.0082 e/Å ²	0.0084 e/Å ²

$\sigma_{\text{hb}} = +0.0082 \text{ e/Å}^2$. All the prominent peaks for the anions, i.e., 0.0085 e/Å^2 for [PF₆], 0.014 e/Å^2 for [CF₃SO₃], 0.015 e/Å^2 for [EtSO₄], and 0.011 e/Å^2 for [BF₄] lie to the right of the cutoff SCD, i.e., $\sigma_{\text{hb}} = +0.0082$. This is due to the inherent negative charge of the anions. The sigma potential is analogous to that observed for cations except that negative values of chemical potentials are encountered on the negative side of the SCDs. The COSMO files generated via GAUSSIAN03 for three cations ([Bmim], [Hmim], [Omim]) and four anions ([PF₆], [BF₄], [CF₃SO₃], [EtSO₄]) can be found in the supplementary material of this manuscript.

Prediction of LLE for Ionic Liquid Systems

COSMO parameters as used earlier, in our work on aromatic extraction of multicomponent systems,³⁰ have been adopted. These are given as COSMO_LL parameters in Table 2 and compared against COSMO-RS parameters of Klamt and Eckert²⁵ as well as against our own COSMO_VL²⁹ parameters. It needs to be emphasized that during COSMO_LL parameter estimation earlier,³⁰ no ionic liquid based system had been taken in the database. LLE for 32 ternary systems, based on 12 different ionic liquids that had already been reported in literature,^{5-9,12-17} has been predicted. Thereafter, LLE has also been predicted for four experimental runs conducted in our own laboratory.

Recent experimental work suggests that ionic liquids can be considered as fully dissociated cations and anions. This fact was used to study the coordination chemistry mechanisms of metal ion extraction, particularly for actinides.⁴³⁻⁴⁵ Experimentally these studies proved that ionic liquids completely dissociate into cations and anions in solution. Also by definition ionic liquid is a liquid with melting point below 100°C containing ions exhibiting ionic conductivity. The fact that the ionic conductivity can be measured experimentally

proves that they consist of ions in solutions. Ionic conductivity studies have been carried out by Carda-Broch et al.⁴⁶ on fluorinated anion like [PF₆].

In molecular dynamic simulations, a cubical box is taken, which contains equal number of cations and anions instead of the composite ionic liquid molecules. For example, in the work of Morrow and Maginn,⁴⁷ the authors studied the thermophysical properties of ionic liquids using 300 cations and 300 anions. Similarly, in the work of Lee et al.,⁴⁸ the ionic conductivity of ionic liquids was found using a cubical box of 100 cations and 100 anions. On the contrary, Rebelo and coworkers³ recently distilled ionic liquid without decomposition at very low pressures. In their pioneering work, they were successful in distilling the [(CF₃SO₂)₂N]-based ionic liquids at 100 Pa and 573 K without decomposition. However, in our method, we are treating ionic liquids in isobaric condition of 1 atm, whereas Rebelo observed the distillation at extremely low pressures. Since the operating pressure for LLE is 1 atm, our approach of considering dissociated cations and anions remains valid.

During VLE predictions of reported ionic-liquid systems,⁴⁹⁻⁵¹ we obtain better results (see Table 3) with dissociation than using a single composite molecule.²⁹ This prompts us to the proposition that the ionic liquid be considered as a dissociated pair of cation and anion for both the VLE and LLE predictions. This novel approach can be applied to ionic liquids containing a limitless combination of cation and anion ($\sim 10^{18}$). Therefore, one has to do quantum mechanical calculations for the cations and anions separately. One can test an ionic liquid for a particular application by addition of sigma profiles and sigma potential of cation and anion only.

Moreover, Klamt and coworkers⁵² have taken recourse to complete equimolar dissociation of ionic liquids into cations and anions for the prediction of infinite dilution activity coefficients using COSMO-RS. In their work, the ionic liquid has

Table 3. Comparison of RMSD for VLE Using the Two Approaches

No.	Ref. no.	System	COSMO-VL	
			Single Molecule ²⁹	Cation and Anion (This Work)
1	49	[Emim] [(CF ₃ SO ₂) ₂ N] + Acetone	.0270	.0181
2	49	[Emim] [(CF ₃ SO ₂) ₂ N] + 2-Propanol	.0380	.0260
3	49	[Emim] [(CF ₃ SO ₂) ₂ N] + Water	.0980	.0526
4	49	[Bmim] [(CF ₃ SO ₂) ₂ N] + Acetone	.0350	.0308
5	49	[Bmim] [(CF ₃ SO ₂) ₂ N] + 2-Propanol	.0400	.0289
6	49	[Bmim] [(CF ₃ SO ₂) ₂ N] + Water	.0980	.0456
7	50	[Mmim] [(CH ₃) ₂ PO ₄] + Acetone	.0510	.0250
8	50	[Mmim] [(CH ₃) ₂ PO ₄] + Tetrahydrofuran	.0460	.0228
9	50	[Mmim] [(CH ₃) ₂ PO ₄] + Water	.1060	.0684
10	50	[Mmim] [(CF ₃ SO ₂) ₂ N] + Benzene	.0892	.0366
11	50	[Mmim] [(CF ₃ SO ₂) ₂ N] + Cyclohexane	.0626	.0423
12	51	[Emim] [EtSO ₄] + Benzene	.0975	.0562
13	51	[Emim] [EtSO ₄] + Cyclohexane	.0694	.0236
Average			.0659	.0366

been taken as an equimolar mixture of two distinct ions: the cation and the anion, which finally contributes to the sigma profile of the mixture as two different compounds.

Assuming complete equimolar dissociation of ionic liquids into cations and anions, we propose the ionic liquid (IL) sigma profile as the linear addition of the sigma profiles of the cation and anion:

$$p_{\text{ionic liquid}}(\sigma) = p_{\text{cation}}(\sigma) + p_{\text{anion}}(\sigma) \quad (1)$$

where $p_{\text{cation}}(\sigma)$ and $p_{\text{anion}}(\sigma)$ are the sigma profiles for cation and anion, respectively.

The mole fraction of ionic liquids can be defined either with respect to two distinct ions or with respect to an ion pair (cation plus anion as one compound). Since the experimental data have been obtained using the latter definition, Klamt and coworkers⁵² scaled the calculated values of γ_i^{inf} by a factor of 0.5. However, in this work, we have obtained the sigma profiles of cation and anion separately and then added them up. After the addition, the sigma profile has been normalized. Thus this profile will behave as if it is a profile of a single molecule. This is equivalent to calculating the sigma profile of a mixture of cation and anion. Along with the sigma profile, the COSMO volumes and areas for the cation and anion also get added linearly. The activity coefficient of the any component in the mixture (here it refers to ionic liquid) is given by²⁷

$$\ln \gamma_{i/S} = n_i \sum_{\sigma} p_i(\sigma) [\ln \Gamma_S(\sigma) - \Gamma_i(\sigma)] + \ln \gamma_{i/S}^{\text{SG}} \quad (2a)$$

Thereafter, the Staverman-Guggenheim (combinatorial contribution) $[\ln \gamma_{i/S}^{\text{SG}}]$ is calculated using the equation:

$$\ln \gamma_{i/S}^{\text{SG}} = \ln \frac{\phi_i}{x_i} + \frac{z}{2} q_i \ln \frac{\theta_i}{\phi_i} + \ln - \frac{\phi_i}{x_i} \sum_j x_j l_j \quad (2b)$$

where

$$\theta_i = \frac{x_i q_i}{\sum_j x_j q_j}, \quad \phi_i = \frac{x_i r_i}{\sum_j x_j r_j}, \quad \text{and} \quad l_i = \frac{z}{2} ((r_i - q_i) - (r_i - 1)) \quad (2c)$$

Here r_i and q_i are normalized using the volume (66.69 Å³) and surface area (79.53 Å²) of a functional group,²⁷ i.e., $r_i = \frac{\text{COSMO Volume}}{66.69}$, $q_i = \frac{\text{COSMO Area}}{79.53}$. Here the COSMO volume and COSMO area are the output from COSMO file.

The goodness of fit for prediction is usually gauged by root mean square deviation (rmsd), which is defined as

$$\text{rmsd (in \%)} = \left[\sum_{k=1}^m \sum_{i=1}^c \sum_{j=1}^2 \frac{(x_{ik}^j - \hat{x}_{ik}^j)^2}{2mc} \right]^{1/2} \quad (3)$$

Here m refers to the number of tie lines, c the number of components, and “2” is the number of phases.

The predicted results for all the reported ionic liquid ternary systems are summarized in Table 4. The 36 data sets contain 12 different ionic liquids comprising of seven different cations and eight anions. Apart from imidazolium based

ionic liquids, pyridinium-based ionic liquid: 1-butyl-3-methylpyridinium tetrafluoroborate [Bmpy] [BF₄] has also been studied. Using the sigma profile for the single composite molecule, it is observed that for nearly half of the systems the values of the activity coefficients were not able to predict the split between the extract (ionic liquid phase) and raffinate phase for the given tie line. Predictions giving an average rmsd of 36.5% and a maximum rmsd of 90% ([Omim] [Cl] – Benzene-Heptane) were observed. No Split (NS) condition for 19 systems was encountered. For another 13 systems, an rmsd ranging from 10 to 90% was observed.

With simple algebraic summation of sigma profiles of cation and anion, we have been able to predict for the first time the LLE of any ionic liquid mixture species. Switching from composite to additive sigma profile, we notice that a NS situation has been converted to a “SPLIT” between the two phases for all the 19 cases. It is clear that the improvement is drastic both for the ionic liquid [Bmim] [CF₃SO₃], [Omim] [MDeg], [Bmpy] [BF₄] systems and also for the alkene-based systems (System nos. 6, 7, 11, 12 of Table 4) for which no prediction had been possible when considering the ionic liquid as a single molecule. For the [Bmim] [CF₃SO₃], [Omim] [MDeg], [Bmpy] [BF₄] systems (System nos. 1, 2, 21, 22, 23–29), the rmsd is less than 10%. Out of the 36 systems studied, most of the predictions are excellent considering the fact that only seven systems gave rmsd greater than 10%. The prediction is excellent considering the fact that no ionic liquid system had been incorporated in the database during the parameter estimation.

Conformational Analysis

Small molecules can have numerous structures or conformers each having equal optimized energy. By rotation around single bonds, molecules with the same molecular formula can form geometrical isomers by arranging their atoms in different, nonequivalent positions; these are called conformers. A conformational analysis needs to be carried out for such molecules. Jork et al.⁵³ obtained the conformers assuming the ions to be in vacuum with their potential energy calculated from a semiempirical method. Then an averaging was carried out over all conformers using a Boltzmann-weighting algorithm. This was then iterated over the occupation numbers of different conformers until consistent results were obtained. Howard and Kollman⁵⁴ gave an excellent overview of the various methods of conformational analysis.

Mullins et al.⁵⁵ obtained the low energy conformers of molecules, which interacted strongly in solutions. For 2-methoxyethanol the conformers were varied manually from the released conformations for further geometry reoptimization. No appreciable change was observed in the sigma profile. Wang et al.⁵⁶ obtained the conformational distribution in sigma profile for 1-hexanol and 2-methoxy-ethanol when the components go from the gas phase to the liquid phase. Vapor and liquid phase ensembles were obtained via configurational-bias Monte Carlo simulations. An average sigma profile for each ensemble was obtained and thereafter was used for thermodynamic property predictions. The difference in sigma profile was only seen in the case of 2-methoxy-ethanol. This difference showed up in the predictions of pure component vapor pressure only. However, VLE predictions

Table 4. Comparison of RMSD for Ternary LLE Using the Two COSMO-LL Approaches

System No.	T (K)	Ref. no.	Systems	Root Mean Square Deviation		
				Single Molecule	Cation + Anion	Exptl. Error
1	298.15	14	[Bmim] [(CF ₃ SO ₃) – Ethanol-Ethyl- <i>tert</i> -Butyl Ether	NS	0.095	NA
2	298.15	12	[Bmim] [(CF ₃ SO ₃) – Ethanol- <i>tert</i> -Amyl Ethyl Ether	NS	0.032	0.0040
3	298.15	8	[Hmim] [BF ₄] – Benzene-Heptane	0.711	0.043	0.0040
4	298.15	8	[Hmim] [BF ₄] – Benzene-Dodecane	0.087	0.098	0.0040
5	298.15	8	[Hmim] [BF ₄] – Benzene-Hexadecane	0.481	0.072	0.0040
6	298.15	16	[Hmim] [BF ₄] – Ethanol-Hexene*	NS	0.147 (0.102) [†]	0.0040
7	298.15	16	[Hmim] [BF ₄] – Ethanol-Heptene	NS	0.125 (0.085) [†]	0.0040
8	298.15	8	[Hmim] [PF ₆] – Benzene-Heptane	0.856	0.042	0.0040
9	298.15	8	[Hmim] [PF ₆] – Benzene-Dodecane	0.3858	0.047	0.0040
10	298.15	8	[Hmim] [PF ₆] – Benzene-Hexadecane	0.457	0.059	0.0040
11	298.15	16	[Hmim] [PF ₆] – Ethanol-Hexene	NS	0.315 (0.115) [†]	0.0040
12	298.15	16	[Hmim] [PF ₆] – Ethanol-Heptene	NS	0.306 (0.125) [†]	0.0040
13	298.15	15	[Omim] [Cl] – Methanol-Hexadecane	0.029	0.005	NA
14	298.15	15	[Omim] [Cl] – Ethanol-Hexadecane	0.030	0.008	NA
15	298.15	13	[Omim] [Cl] – Ethanol- <i>tert</i> -Amyl Ethyl Ether	0.382	0.067	NA
16	298.15	9	[Omim] [Cl] – Benzene-Heptane	0.896	0.096	0.0060
17	298.15	9	[Omim] [Cl] – Benzene-Dodecane	0.058	0.096	0.0060
18	298.15	9	[Omim] [Cl] – Benzene-Hexadecane	0.146	0.070	0.0060
19	298.15	5	[Emim] [C ₈ H ₁₇ SO ₄] – Benzene-Heptane	0.362	0.070	0.0060
20	298.15	5	[Emim] [C ₈ H ₁₇ SO ₄] – Benzene-Hexadecane	0.456	0.140	0.0060
21	298.15	5	[Omim] [MDEG] – Benzene-Heptane	NS	0.103	0.0060
22	298.15	5	[Omim] [MDEG] – Benzene-Hexadecane	NS	0.043	0.0060
23	313.15	6	[Bmpy] [BF ₄] – Xylene-Octane	NS	0.030	0.0025
24	348.15	6	[Bmpy] [BF ₄] – Xylene-Octane	NS	0.024	0.0025
25	313.15	6	[Bmpy] [BF ₄] – Ethylbenzene-Octane	NS	0.041	0.0025
26	348.15	6	[Bmpy] [BF ₄] – Ethylbenzene-Octane	NS	0.029	0.0025
27	313.15	6	[Bmpy] [BF ₄] – Benzene-Hexane	NS	0.048	0.0025
28	333.15	6	[Bmpy] [BF ₄] – Benzene-Hexane	NS	0.036	0.0025
29	298.15	6	[Bmpy] [BF ₄] – Toluene-Heptane	NS	0.075	0.0025
30	298.15	7	[Mmim] [CH ₃ SO ₄] – Toluene-Heptane	0.455	0.008	0.0025
31	298.15	7	[Emim] [C ₂ H ₅ SO ₄] – Toluene-Heptane	0.116	0.031	0.0025
32	298.15	7	[Bmim] [CH ₃ SO ₄] – Toluene-Heptane	0.235	0.032	0.0025
33	313.15	This work	[Emim] [EtSO ₄] – Ethanol-Hexene	NS	0.124	0.005
34	313.15	This work	[Emim] [EtSO ₄] – Ethanol-Heptene	NS	0.023	0.005
35	313.15	This work	[E-2,3-dmim] [EtSO ₄] – Ethanol-Hexene	NS	0.032	0.005
36	313.15	This work	[E-2,3-dmim] [EtSO ₄] – Ethanol-Heptene	NS	0.065	0.005
Average RMSD deviation				0.365	0.096	0.004
Average RMSD deviation (with conformer) [†]					0.066	

NS: no splitting of the phase; NA: not available; MDEG: monomethyldiethyleneglycol.

Values in bold indicate deviations greater than 10%.

*Benchmarked for validation with experimental procedure.

[†]Indicates sigma profile correction by 1.23 due to alkene conformers.

with mixtures containing 1-hexanol showed little difference in phase equilibria, whereas mixtures with 2-methoxy-ethanol showed noticeable but not significant difference in phase equilibria predictions

We have applied the conformational approach to ternary systems containing alkenes, since for all the four systems containing alkenes (System nos. 6, 7, 11, 12 of Table 4) the rmsd predicted is quite high (~23% in rmsd). A conformational analysis on the alkene molecule is performed similar to our previous work on multicomponent aromatic extraction systems.^{30,57} To improve the prediction for systems containing alkenes, we have adopted a conformer correction in the sigma profile of alkenes. However, it should be kept in mind that there is no literature data regarding what percentage of each conformer/structure contributes to the solution.

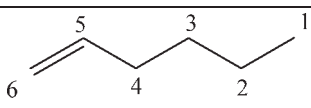
The conformers of alkenes are obtained by the same procedure as reported by Fraser et al.⁵⁸ for 1-pentene. The five conformers with the dihedral angles, i.e., C1—C2—C3—C4 and C2—C3—C4—C5 are shown in Table 5; here C1 represents the carbon atom of the terminal methyl group. The

value of corrected sigma profile obtained was found to be $p(\sigma)_{\text{av,alkene}} \sim 1.23 \times p(\sigma)_{\text{alkene}}$, where $p(\sigma)_{\text{av,alkene}}$ is the sigma profile averaged over the five different conformers of alkenes. As in the case with nonionic liquid systems, the overall deviations came down to 10.6%. The results are significantly better with the corrected sigma profile of alkene. After applying conformational correction the average rmsd drops from 22.6% to 10.6% for alkene-based systems and the overall rmsd drops from 9.6% to 6.6%. These values are excellent when compared with the average rmsd value of 36.5% for the ionic liquid taken as a single composite molecule.

Experimentation

Chemicals

The ionic liquids: 1-hexyl-3-methylimidazolium tetrafluoroborate [Hmim] [BF₄] (used as a benchmarking system), 1-ethylimidazolium ethylsulphate [Emim] [EtSO₄], and 1-ethyl-2,3-dimethylimidazolium ethylsulphate [E-2,3dmim] [EtSO₄] were purchased from Fluka; each having a reported water

Table 5. Dihedral Angles for Five Conformers of 1-Hexene


	Dihedral (1-2-3-4)	Dihedral (2-3-4-5)
Conformer 1	-120	180
Conformer 2	-120	60
Conformer 3	120	60
Conformer 4	0	180
Conformer 5	0	60

content of 0.1% (mass). Ethanol (99%), hexene (99.5%), heptene (98.5%) had been purchased from Lancaster. Prior to use, the ionic liquids had been dried at 1 mm Hg for 24 h at 353 K. After drying the water, content in ILs was expected to be much less than 0.1% (mass). The organic solutes were used without any further purification. The purity of ethanol and hexene was confirmed through gas chromatography, which showed absence of any other significant peak.

Procedure

To carry out LLE experiments the feed samples were made up of the desired composition of the components such that a two-phase split could occur. The phase compositions were measured using a mass balance (PD Scientific make, ± 0.001 g). The mixtures were inserted inside a glass flask of 20 ml volume, covered by open-top lids sealed with combined silicone/Teflon septa. These flasks were then placed in a thermostatic bath (Mahendra Scientific Make) with a coupled multistirring plate to stir the samples and keep the temperature of the bath to an accuracy of ± 0.1 K. The shaker was operated at a speed of about 250–350 rpm. Spring clamps were used to hold the flasks on the tray. All the mixtures were vigorously stirred for 4 h and then allowed to settle for no less than 12 h to ensure equilibrium state. Unlike other systems, tie lines could not be estimated via gas chromatography, ionic liquid being a nonvolatile component. NMR spectroscopy, however, is currently a viable option for estimating the tie lines for ionic liquid systems. Earlier, Arce et al.^{12,13} had measured the tie lines for the ionic liquids: [Bmim] [CF₃SO₃] and [Omim] [Cl]. In a subsequent work, Arce et al.^{17–19} measured the tie lines for the ternary system containing [Emim] [EtSO₄] and 1-ethyl-3-methyl imidazoliumbis{(trifluoromethyl) sulfonyl}amide [Emim] [(CF₃SO₃)₂N].^{10,11} For the analysis part, a sample of each layer was withdrawn using glass syringes with coupled stainless steel needles. A drop of each sample was dissolved in 0.5 ml of CDCl₃ (Aldrich, 99.8% deuterated) and placed inside NMR-tubes (Royal Imperial Grade) which were properly sealed. The NMR spectrometer of 11.74 T (400 MHz resonance for ¹H) was used to measure the peaks.

Quantitative analysis

First the NMR technique was tested on known mass composition. Known mass composition mixtures were prepared and a drop of each of the mixture was dissolved in 0.5 ml of CDCl₃ and introduced into the NMR-tubes. Then the analysis

was performed on the NMR spectrometer, with 15 scans and a relaxation time of 25 s. Table 6 shows the peak assignment in the ¹H NMR spectrum of the ternary system, the structure of the molecules, and the correspondence between hydrogen positions and peaks.

Alkenes are the most easy to identify because of their double bonds and they lie in between 5 and 6 δ , relative to TMS. For ethanol the —OH peak is very difficult to locate so we chose to identify the —CH₂ peak for analysis as it is easily observable as a quartet and lies at ~ 4 δ in the spectra. For all the ionic liquids, the peaks suitable for integration are only of the cation. For the ionic liquid, the imidazolium ring protons all lie in the vicinity of 7 to 9 δ (a, b in Table 6). So all the three protons have been taken for quantitative analysis. Peak areas are proportional to hydrogen moles associated with the referred component. Thus, dividing the peak area by the number of hydrogen atoms we obtain an area proportional to the moles of the referred component. Finally, the molar fraction is obtained by dividing this area by the total sum of the areas of the three components. In this way, calculated compositions are independent of sample size. The standard deviations of the fits, in molar fraction, were found to be 0.004 for hexene and 0.005 for ethanol and the ionic liquid.

Benchmarking

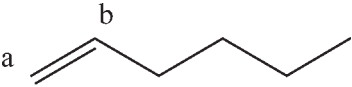
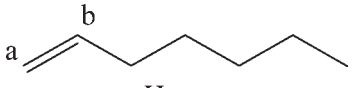
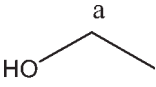
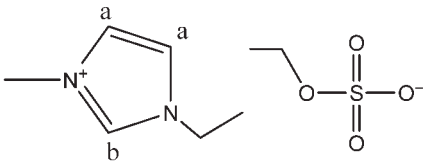
For benchmarking we took the experimental results of Letcher and Reddy¹⁶ for the system: [Hmim] [BF₄] – Ethanol-hexene. We benchmarked this system so as to carry out a similar work related to alkene-alcohol separation. Four single batch experiments were conducted for this system under similar conditions as described in the analysis. The experimental and measured tie lines are compared and reported in Table 7. Overall feed compositions were taken corresponding to the center of the reported tie lines. Sample from the raffinate and extract phases were collected at the end of experiment as described earlier. The experimental compositions were then obtained by integrating the peaks of the NMR spectra. The percent root mean square deviation (rmsd) for these four tie lines came out to be 8.43%.

There are significant differences in the reported and experimental data for the ethanol concentrations in the raffinate phase. The method of analysis using NMR spectroscopy has an inherent error based on the frequency of magnetic field (i.e., 400 MHz) and its strength (11.74 T). The raffinate phase consists mainly of ethanol and hexene along with negligible amount of ionic liquid. This high difference is due to the inaccurate integration of either hexene or ethanol peak, since the combined mole fraction of hexene and ethanol matches with that of literature. A detailed analysis needs to be carried out. The NMR spectrum of the ionic liquid rich phase is given in the supplementary material of this article.

Separation of alkene-ethanol

The Fischer-Tropsch process for the production of transport fuel from carbon monoxide or coal, produces a range of oxygenates and hydrocarbons including a range of alkanols and olefins. The separation of ethanol from olefins is of particular interest to this industry; so we decided to address the problem of alkene-alcohol separation. Having confirmed the reliability of the experimental procedure and quantitative

Table 6. Peak Assignment for Quantitative Analysis of NMR for Ternary Mixture

Chemical Compound and Peak Type	Chemical Shifts in NMR Spectra (Relative to TMS)
 Hexene	a: ~5 (quintuplet, 2 H) b: 5.8 (quintuplet, 1 H)
 Heptene	a: 5.2 (quintuplet, 2 H) b: 5.9 (quintuplet, 1 H)
 Ethanol	a: ~3.5 (quartet, 2 H)
 1-Ethyl-3-methylimidazolium ethylsulphate	a: ~7.3 (doublet, 2 H) b: ~8.9 (doublet, 1 H)

analysis, the experiments for ternary systems with pure solvents comprising of components from alkene series (Hexene, Heptene), one component from alcohol series (Ethanol) and the ionic liquid ([Emim] [EtSO₄], [E-2,3dmim] [EtSO₄]) were conducted in multibatch fashion. System nos. 33–36 of Table 4 were chosen for this purpose. Feed samples were made of desired compositions of the components such that it splits into two phases. Eight feed samples corresponding to each ternary system were prepared and run in a multibatch fashion. The amounts of the various components in the feed samples along with the tie line compositions for these four systems are given in Table 8. Graphical representations of the tie lines are shown for the systems: [Emim] [EtSO₄] – Ethanol–

heptene in Figure 5, [Emim] [EtSO₄] – Ethanol–Heptene in Figure 6, [E-2,3-dmim] [EtSO₄] – Ethanol–Hexene in Figure 7, and [E-2,3-dmim] [EtSO₄] – Ethanol–Heptene in Figure 8.

COSMO_LL prediction

After having successfully determined the experimental tie lines for four ternary systems, predictions using COSMO_LL model are shown in Figures 5–8 for our measured systems. From Table 4, it can be seen that except for [Emim] [EtSO₄] – Ethanol–Hexene (System no. 33), the a priori predictions for other systems (System nos. 34–36) are excellent when compared with the experimental values.

Table 7. Comparison of Experimental and Reported Tie Lines for the System [Hmim] [BF₄] – Ethanol–Hexene at 25°C

Tie line		Extract Phase (Mole Fraction)			Raffinate Phase (Mole Fraction)		
		[Hmim] [BF ₄]	Ethanol	Hexene	[Hmim] [BF ₄]	Ethanol	Hexene
2	Reported*	0.681	0.199	0.120	0.000	0.016	0.984
	Expt.	0.675	0.213	0.112	0.000	0.001	0.999
4	Reported*	0.542	0.308	0.150	0.000	0.031	0.969
	Expt.	0.545	0.341	0.114	0.000	0.001	0.999
7	Reported*	0.450	0.414	0.136	0.001	0.119	0.880
	Expt.	0.404	0.477	0.119	0.000	0.002	0.998
10	Reported*	0.280	0.577	0.143	0.002	0.330	0.668
	Expt.	0.274	0.581	0.145	0.000	0.009	0.991
rmsd = 0.0843							

*Ref. 16.

Table 8. Experimental Tie lines, Selectivities, and Distribution Ratios for IL Systems

A [Emim] [EtSO ₄] – Ethanol-Hexene at 313.15 K								
Tie Line	Extract Phase			Raffinate Phase			Selectivity	Solute Distribution Ratio
	(Mole Fraction)			(Mole Fraction)				
	IL	Ethanol	Hexene	IL	Ethanol	Hexene		
1	0.884	0	0.116	0	0	1	–	–
2	0.826	0.061	0.113	0	0.04	0.96	1931.5	1.53
3	0.785	0.104	0.111	0.012	0.06	0.928	1343.6	1.73
4	0.744	0.148	0.109	0.016	0.08	0.904	332.6	1.85
5	0.703	0.19	0.107	0.08	0.104	0.816	270.6	1.83
6	0.673	0.222	0.105	0.12	0.152	0.728	262.6	1.46
7	0.638	0.258	0.104	0.19	0.185	0.625	248.2	1.39
8	0.59	0.315	0.095	0.223	0.214	0.563	407.1	1.47
[Emim] [EtSO ₄] – Ethanol-Heptene at 313.15 K								
B	IL	Ethanol	Heptene	IL	Ethanol	Heptene		
1	0.9266	0	0.0735	0	0.012	0.988	–	–
2	0.865	0.0637	0.0712	0	0.0236	0.9764	37.01	0.00
3	0.8214	0.1089	0.0697	0	0.086	0.914	16.61	2.70
4	0.7774	0.1544	0.0683	0	0.141	0.859	13.77	1.27
5	0.7348	0.1982	0.067	0	0.189	0.811	12.69	1.10
6	0.7022	0.2318	0.066	0	0.245	0.755	10.82	1.05
7	0.6662	0.2688	0.065	0	0.289	0.711	10.17	0.95
8	0.6305	0.3054	0.0641	0	0.302	0.698	11.01	0.93
[E-2,3dmim] [EtSO ₄] – Ethanol-Hexene at 313.15 K								
	IL	Ethanol	Hexene	IL	Ethanol	Hexene		
1	0.9169	0	0.0831	0.0003	0	0.9997	–	–
2	0.7518	0.1183	0.1299	0.0003	0.003	0.9967	302.6	39.43
3	0.6283	0.2213	0.1504	0.0002	0.0119	0.9879	122.2	18.60
4	0.5261	0.3032	0.1707	0.0005	0.0097	0.9898	181.2	31.26
5	0.4906	0.3277	0.1817	0.0003	0.0102	0.9895	175	32.13
6	0.4558	0.3417	0.2025	0.0003	0.0133	0.9864	125.1	25.69
7	0.4306	0.359	0.2104	0.0003	0.0128	0.9869	131.6	28.05
8	0.3635	0.4109	0.2256	0.0003	0.0195	0.9802	91.6	21.07
[E-2,3dmim] [EtSO ₄] – Ethanol-Heptene at 313.15 K								
	IL	Ethanol	Heptene	IL	Ethanol	Heptene		
1	0.98	0	0.02	0.022	0.0065	0.9715	–	–
2	0.927	0.035	0.038	0.007	0.0309	0.9621	28.68	0.00
3	0.906	0.045	0.049	0.01	0.0143	0.9757	62.66	1.13
4	0.885	0.055	0.06	0.011	0.0116	0.9774	77.24	3.15
5	0.822	0.081	0.097	0.006	0.0122	0.9818	67.2	4.74
6	0.756	0.11	0.134	0.008	0.016	0.976	50.07	6.64
7	0.691	0.139	0.17	0.006	0.0154	0.9786	51.96	6.88
8	0.356	0.25	0.394	0.021	0.0234	0.9556	25.91	9.03

Interpretation of tie line behavior

An examination of the slope of the tie lines is significant in determining the separating capability of the ionic liquids. As can be observed in Figures 5–8, there is a similar sloping behavior of the tie lines for the two ionic liquid systems. This is important for a comparative study of the effect of the nature of the cation on the separation efficiency of ionic liquids for specific mixtures. For the [Emim] [EtSO₄] + ethanol + an alkene systems, the sloping of the tie lines toward the ethanol vertex indicates that ethanol is more soluble in ionic liquid rich layer than in the alkene rich layer. This is indeed favorable for the extraction of ethanol from ethanol-alkene mixtures into the ionic liquid-rich phase. For selective

liquid–liquid extraction of ethanol from an alkene, the use of ionic liquids containing sulphate anions would be favorable. A similar observation was observed for [Hmim] [BF₄] as a solvent¹⁶ for separating alcohol and alkene.

The ability of the ionic liquid to separate the ethanol-alkene mixtures can be found out by calculating the selectivity values (Eq. 4a) and solute distribution ratio (Eq. 4b) from the tie line, as given by

$$S = \frac{\left(\frac{x_{\text{alcohol}}}{x_{\text{alkene}}} \right)_{\text{Ionic Liquid Phase}}}{\left(\frac{x_{\text{alcohol}}}{x_{\text{alkene}}} \right)_{\text{Alkene Rich Phase}}} \quad (4a)$$

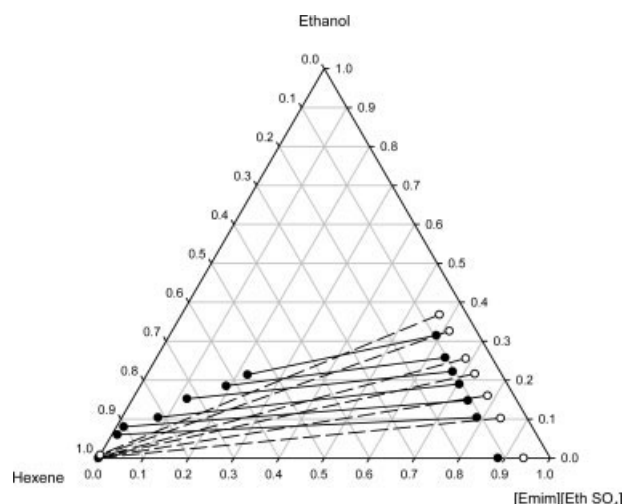


Figure 5. Experimental and COSMO_LL predicted tie lines for [Emim] [EtSO₄] – Ethanol-Hexene at 313.15 K.

$$\beta = \left(\frac{x_{\text{ethanol}}^{\text{IL Rich Phase}}}{x_{\text{ethanol}}^{\text{alkene rich phase}}} \right) \quad (4b)$$

The selectivity value, S , as described previously confirms the extraction efficiencies for both the ionic liquids. From Figures 9 and 10, the selectivity values are highest for [Hmim] [BF₄] for heptene-ethanol separation and [Emim] [EtSO₄] for hexene-ethanol systems. The selectivities for [Emim] [EtSO₄] in separating hexene and ethanol are ~13 times greater than those measured for [Hmim] [BF₄].¹⁶ The

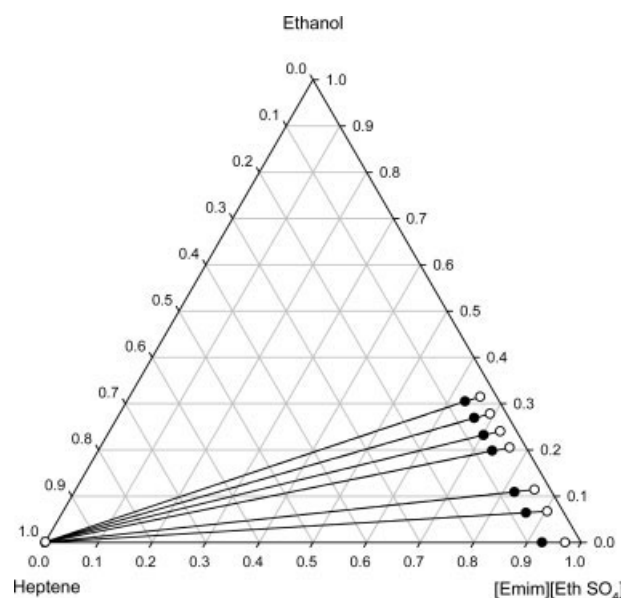


Figure 6. Experimental and COSMO_LL predicted tie lines for [Emim] [EtSO₄] – Ethanol-Heptene at 313.15 K.

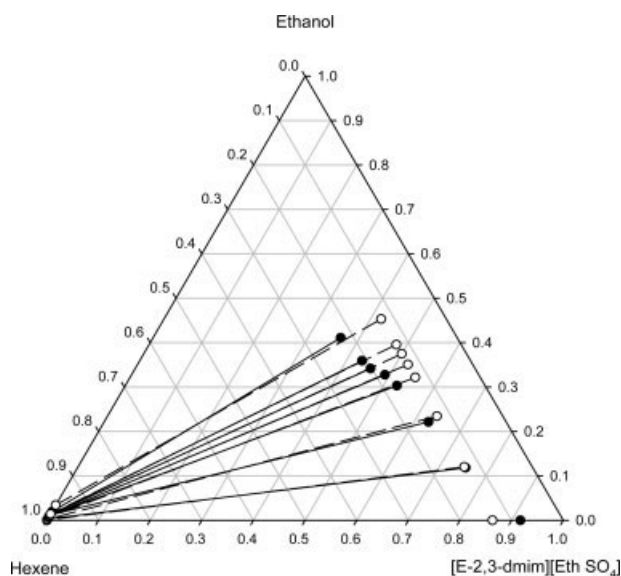


Figure 7. Experimental and COSMO_LL predicted tie lines for [E-2,3-dmim] [EtSO₄] – Ethanol-Hexene at 313.15 K.

selectivity and solute distribution ratio values are also reported in Table 8.

Conclusion

The effect of ionic liquid dissociating into cations and anions has been handled by a linear combination of sigma profiles for the LLE prediction. This novel approach can be applied to ionic liquids containing a limitless combination of cation and anion ($\sim 10^{18}$). For this, one has to do a quantum mechanical calculation for the cations and anions separately and then test an ionic liquid for a particular application. Thereafter COSMO_LL model has been validated on 32 ter-

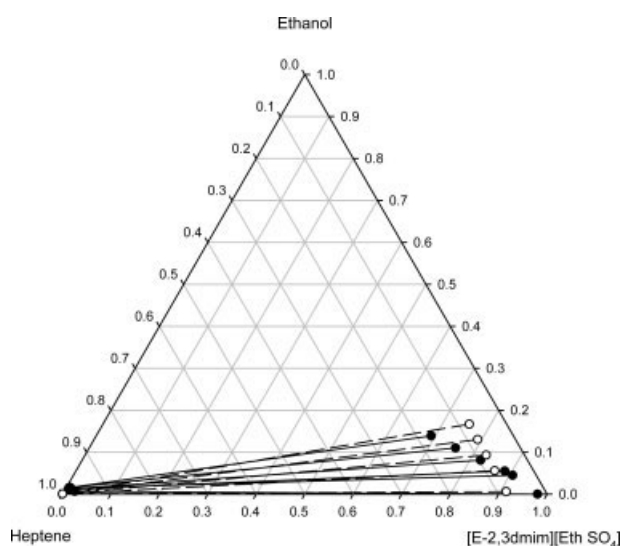


Figure 8. Experimental and COSMO_LL predicted tie lines for [E-2,3dmim] [EtSO₄] – ethanol-heptene at 313.15 K.

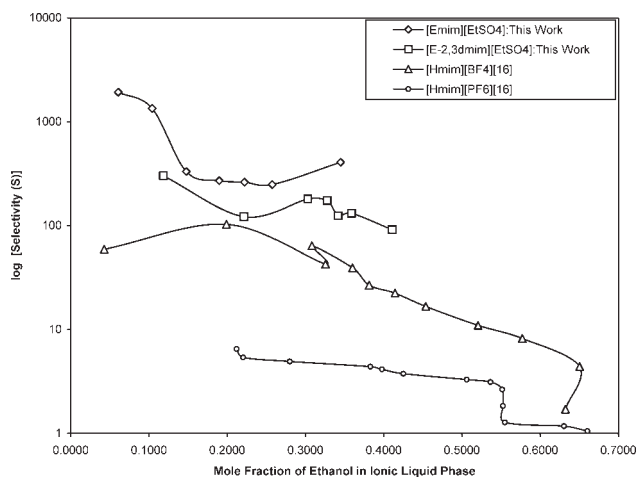


Figure 9. Selectivity (S) as a function of mole fraction of ethanol for various ionic liquids for the separation of hexene-ethanol.

nary ionic liquid systems. Additionally, experimental studies have been carried out for the separation of alkene and ethanol using ionic liquid as a solvent. COSMO_LL has also been used to validate our experimental results on the four new ionic liquid systems. In this process, LLE data have been generated for the four new ternary ionic liquid systems. Conformational corrections for alkene have been used to improve the prediction of alkenes-based systems.

Notation

Symbols

- m = number of tie lines
- C = number of components
- SCD = screening charge densities, $e/\text{\AA}^2$
- px = probability distribution of SCDs
- x = mole fraction in liquid phase

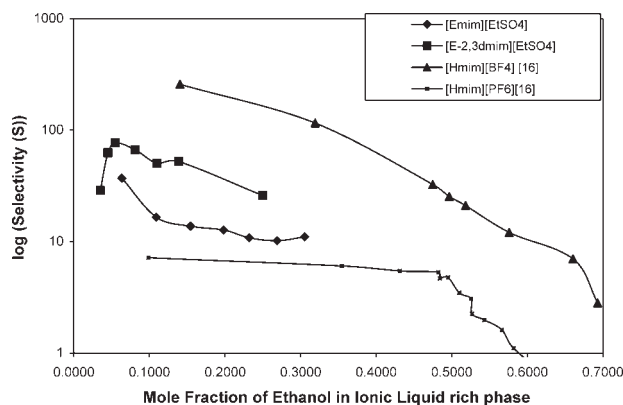


Figure 10. Selectivity (S) as a function of mole fraction of ethanol for various ionic liquids for the separation of heptene-ethanol.

T = temperature, K
 u^x = sigma potential for pure component "x," kJ/(mol \AA^2)

Greek letters

- σ = SCD, $e/\text{\AA}^2$
- σ_{hb} = cutoff SCD for hydrogen bonding, $e/\text{\AA}^2$
- $\Gamma_i(\sigma)$ = segment activity coefficient for pure component i
- $\Gamma_S(\sigma)$ = segment activity coefficient for mixture, S
- γ_s^i = component activity coefficient in the mixture, S

Literature Cited

- Brennecke JF, Magninn EJ. Ionic liquids: innovative fluids for chemical processing. *AIChE J.* 2001;47:2384–2389.
- Rogers RD, Huddleston JG, Willauer HD, Swatoski RP, Visser AE. Room temperature ionic liquids as novel media for clean liquid-liquid extraction. *Chem Commun.* 1998;1765–1766.
- Earle MJ, Esperanca JMMSS, Gilea MA, Lopes JNC, Rebelo LPN, Magee JW, Seddon KR, Widegren JA. The distillation and volatility of ionic liquids. *Nature* 2006;439:831–834.
- Heintz A. Recent developments in thermodynamics and thermophysics of non-aqueous mixtures containing ionic liquids. A review. *J Chem Thermodyn.* 2005;37:525–535.
- Deenadayalu N, Ngcongco CN, Letcher TM, Ramjugernath D. Liquid-liquid equilibria for ternary mixtures (an ionic liquid + benzene + heptane or hexadecane at $T = 298.2$ K and atmospheric pressure. *J Chem Eng Data.* 2006;51:988–991.
- Meindersma GW, Podt A, Haan AB. Ternary liquid-liquid equilibria for mixtures of an aromatic + an aliphatic hydrocarbon + 4-methyl-*N*-butylpyridinium tetrafluoroborate. *J Chem Eng Data* 2006;51:1814–1819.
- Meindersma GW, Podt A, Haan AB. Ternary liquid-liquid equilibria for mixtures of toluene + *n*-heptane + an ionic liquid. *Fluid Phase Equilib.* 2006;247:158–168.
- Letcher TM, Reddy P. Ternary (liquid + liquid) equilibria for mixtures of 1-hexyl-3-methylimidazolium (tetrafluoroborate or hexafluorophosphate + benzene + an alkane at $T = 298.2$ K and $p = 0.1$ MPa. *J Chem Thermodyn.* 2005;37:415–421.
- Letcher TM, Deenadayalu N. Ternary liquid-liquid equilibria for mixtures of 1-methyl-3-octyl-imidazolium chloride + benzene + an alkane at $T = 298.2$ K and 1 atm. *J Chem Thermodyn.* 2003;35:67–76.
- Arce A, Earle MJ, Rodríguez H, Seddon KR. Separation of aromatic hydrocarbons from alkanes using the ionic liquid 1-ethyl-3-methylimidazolium bis((trifluoromethyl) sulfonyl)amide. *Green Chem.* 2007;1:70–74.
- Arce A, Earle MJ, Rodríguez H, Seddon KR. Separation of benzene and hexane by solvent extraction with 1-alkyl-3-methylimidazolium bis((trifluoromethyl)sulfonyl)amide ionic liquids: effect of the alkyl-substituent length. *J Phys Chem B.* 2007;111:4732–4736.
- Arce A, Rodriguez O, Soto A. *tert*-Amyl ethyl ether separation from its mixtures with ethanol using the 1-butyl-3-methylimidazolium trifluoromethanesulfonate ionic liquid: liquid-liquid equilibrium. *Ind Eng Chem Res.* 2004;43:8323–8327.
- Arce A, Rodriguez O, Soto A. Experimental determination of liquid-liquid equilibrium using ionic liquids: *tert*-amyl ethyl ether + ethanol + 1-octyl-3-methylimidazolium chloride system at 298.15 K. *J Chem Eng Data* 2004;49:514–517.
- Arce A, Rodriguez O, Soto A. Purification of ethyl *tert*-butyl ether from its mixtures with ethanol by using an ionic liquid. *Chem Eng J.* 2006;115:219–223.
- Letcher TM, Deenadayalu N, Soko B, Ranjugernath D, Naicker PK. Ternary liquid-liquid equilibria for mixtures of 1-methyl-3-octylimidazolium chloride + an alkanol + an alkane at 298.2 K and 1 bar. *J Chem Eng Data* 2003;48:904–907.
- Letcher TM, Reddy P. Ternary liquid-liquid equilibria for mixtures of 1-hexyl-3-methylimidazolium (tetrafluoroborate or hexafluorophosphate) + ethanol + an alkane at $T = 298.2$ K. *Fluid Phase Equilib.* 2004;219:107–112.
- Arce A, Marchiaro A, Rodríguez O, Soto A. Citrus essential oil terpenes by liquid-liquid extraction using organic solvents or ionic liquids. *AIChE J.* 2006;52:2089–2097.

18. Arce A, Pobudkowska A, Rodríguez O, Soto A. Citrus essential oil terpenes by extraction using 1-ethyl-3-methylimidazolium ethylsulfate ionic liquid: effect of the temperature. *Chem Eng J*. 2007;133: 213–218.
19. Arce A, Rodríguez H, Soto A. Use of a green and cheap ionic liquid to purify gasoline octane boosters. *Green Chem*. 2007;3:247–253.
20. Renon H, Prausnitz JM. Local compositions in thermodynamic excess functions for liquid mixtures. *AIChE J*. 1968;14:135–144.
21. Abrams DS, Prausnitz JM. Statistical thermodynamics of liquid mixtures. New expression for the excess Gibbs energy of partly or completely miscible systems. *AIChE J*. 1975;21:116–128.
22. Klamt A, Schüürmann G. COSMO: a new approach to dielectric screening in solvents with explicit expressions for the screening energy and its gradient. *J Chem Soc Perkin Trans 2* 1993;799–805.
23. Klamt A. Conductor like screening model for real solvents: a new approach to the quantitative calculation of solvation phenomena. *J Phys Chem*. 1995;99:2224–2235.
24. Klamt A, Eckert F. COSMO-RS: a novel and efficient method for the a priori prediction of thermophysical data of liquids. *Fluid Phase Equilib*. 2000;172:43–72.
25. Klamt A, Eckert F. Fast solvent screening via quantum chemistry: COSMO-RS approach. *AIChE J*. 2002;48:369–385.
26. Klamt A. *COSMO-RS: From Quantum Chemistry to Fluid Phase Thermodynamics and Drug Design*, 1st ed. Amsterdam: Elsevier, 2005.
27. Lin S, Sandler SI. A priori phase equilibrium prediction from a segment contribution solvation model. *Ind Eng Chem Res*. 2002;41: 899–913.
28. Gmehling H, Gmehling J. Performance of a conductor like screening model for real solvents model in comparison to classical group contribution methods. *Ind Eng Chem Res*. 2005;44:1610–1624.
29. Banerjee T, Singh MK, Khanna A. Prediction of binary VLE for imidazolium based ionic liquid systems using COSMO-RS. *Ind Eng Chem Res*. 2006;45:3207–3219.
30. Banerjee T, Sahoo RK, Khanna A. Multi-component liquid-liquid equilibria prediction for aromatic extraction systems using COSMO-RS. *Ind Eng Chem Res*. 2007;46:1292–1304.
31. Banerjee T, Khanna A. Infinite dilution activity coefficients for trihexyltetradecyl phosphonium ionic liquids: measurements and COSMO-RS prediction. *J Chem Eng Data*. 2006;51:2170–2177.
32. Domanska U, Pobudkowska A, Eckert F. Liquid-liquid equilibria in the binary systems (1,3-dimethylimidazolium, or 1-butyl-3-methylimidazolium methylsulfate + hydrocarbons). *Green Chem*. 2006;8: 268–276.
33. Frisch MJ, Trucks GW, Schlegel HB, Scuseria GE, Robb MA, Cheeseman JR, Montgomery JA Jr, Vreven T, Kudin KN, Burant JC, Millam JM, Iyengar SS, Tomasi J, Barone V, Mennucci B, Cossi M, Scalmani G, Rega N, Petersson GA, Nakatsuji H, Hada M, Ehara M, Toyota K, Fukuda R, Hasegawa J, Ishida M, Nakajima T, Honda Y, Kitao O, Nakai H, Klene M, Li X, Knox JE, Hratchian HP, Cross JB, Adamo C, Jaramillo J, Gomperts R, Stratmann RE, Yazyev O, Austin AJ, Cammi R, Pomelli C, Ochterski JW, Ayala PY, Morokuma K, Voth GA, Salvador P, Dannenberg JJ, Zakrzewski VG, Dapprich S, Daniels AD, Strain MC, Farkas O, Malick DK, Rabuck AD, Raghavachari K, Foresman JB, Ortiz JV, Cui Q, Baboul AG, Clifford S, Cioslowski J, Stefanov BB, Liu G, Liashenko A, Piskorz P, Komaromi I, Martin RL, Fox DJ, Keith T, Al-Laham MA, Peng CY, Nanayakkara A, Challacombe M, Gill PMW, Johnson B, Chen W, Wong MW, Gonzalez C, Pople JZ. *Gaussian 03*. Pittsburgh PA: Gaussian, Inc., 2003.
34. Perdew JP. Density-functional approximation for the correlation energy of the inhomogeneous electron gas. *Phys Rev B*. 1986;33: 8822–8824.
35. Schaefer A, Huber C, Ahlrichs R. Fully optimized contracted Gaussian basis sets of triple zeta valence quality for atoms Li to Kr. *J Chem Phys*. 1994;100:5829–5835.
36. Sosa C, Andzelm J, Elkin BC, Wimmer E, Dobbs KD, Dixon DA. A local density functional study of the structure and vibrational frequencies of molecular transition-metal compounds. *J Phys Chem*. 1992;96:6630–6636.
37. Bondi A. van der Waals volumes and radii. *J Phys Chem*. 1964;68:441–451.
38. Bondi A. *Physical Properties of Molecular Crystals, Liquids and Glasses*. New York: Wiley, 1968.
39. Fock V. *Z Physik*. 1930;61:126.
40. Turner EA, Pye C, Singer RD. Use of ab initio calculations toward the rational design of room temperature ionic liquids. *J Phys Chem A*. 2003;107:2277–2288.
41. Meng J, Dolle A, Carper RW. Gas phase model of an ionic liquid: semi-empirical and ab-initio bonding and molecular structure. *J Mol Struct (Theochem)*. 2002;585:119–128.
42. Schaftenaar G, Noordik JH. Molden: a pre- and post-processing program for molecular and electronic structures. *J Comput Aided Mol Des*. 2000;14:123–134.
43. Cocalia VA, Gutowski KE, Rogers RD. The coordination chemistry of actinides in ionic liquids: a review of experiment and simulation. *Coord Chem Rev*. 2006;250:755–764.
44. Jensen MP, Neufeind J, Beitz JV, Skanthakumar S, Soderholm L. Mechanisms of metal ion transfer into room-temperature ionic liquids: the role of anion exchange. *J Am Chem Soc*. 2003;125: 15466–15473.
45. MacFarlane DR, Seddon KR. Ionic liquids-progress on the fundamental issues. *Aust J Chem*. 2007;60:3–5.
46. Carda-Broch S, Berthod A, Armstrong DW. Solvent properties of the 1-butyl-3-methylimidazolium hexafluorophosphate ionic liquid. *Anal Bioanal Chem*. 2003;375:191–199.
47. Morrow TI, Maginn EJ. Molecular dynamics study of the ionic liquid 1-n-butyl-3-methylimidazolium hexafluorophosphate. *J Phys Chem B*. 2002;106:12807–12813.
48. Lee SU, Jung J, Han Y. Molecular dynamics study of the ionic conductivity of 1-n-butyl-3-methylimidazolium salts as ionic liquids. *Chem Phys Lett*. 2005;406:332–340.
49. Doker M, Gmehling J. Measurement and prediction of vapor-liquid equilibria of ternary systems containing ionic liquids. *Fluid Phase Equilib*. 2005;225:255–266.
50. Kato R, Gmehling J. Measurement and correlation of vapor-liquid equilibria of binary systems containing the ionic liquids [EMIM][CF₃SO₂]₂N], [Bmim][CF₃SO₂]₂N], [MMIM][CH₃]₂PO₄] and oxygenated organic compounds respectively water. *Fluid Phase Equilib*. 2005;231:38–43.
51. Kato R, Krummen M, Gmehling J. Measurement and correlation of vapor-liquid equilibria and excess enthalpies of binary systems containing ionic liquids and hydrocarbons. *Fluid Phase Equilib*. 2004;224:47–54.
52. Diedenhofen M, Eckert F, Klamt A. Prediction of infinite dilution activity coefficients of organic compounds in ionic liquids using COSMO-RS. *J Chem Eng Data* 2003;48:475–479.
53. Jork C, Kristen C, Pieraccini D, Stark A, Chiappe C, Beste YA, Arlt W. Tailor-made ionic liquids. *J Chem Thermodyn*. 2005;37:537–558.
54. Howard AE, Kollman PA. An analysis of current methodologies for conformational searching of complex molecules. *J Med Chem*. 1988;31:1669–1675.
55. Mullins E, Oldland R, Liu YA, Wang S, Sandler SI, Chen CC, Zwolak M, Seavey KC. Sigma-profile database for using COSMO-based thermodynamic methods. *Ind Eng Chem Res*. 2006;45:4389–4415.
56. Wang S, Stubbs JM, Siepmann JI, Sandler SI. Effects of conformational distributions on sigma profiles in COSMO theories. *J Phys Chem A*. 2005;109:11285–11294.
57. Sahoo RK, Banerjee T, Khanna A. UNIQUAC interaction parameters with closure for imidazolium based ionic liquid systems using genetic algorithm. *Can J Chem Eng*. 2007;85:833–853.
58. Fraser GT, Xu HL, Suenram RD, Lugez LC. Rotational spectra of four of the five conformers of 1-pentene. *J Chem Phys*. 2000;112: 6209–6217.

Manuscript received Jun. 5, 2007, and revision received Feb. 19, 2008.